Temperature dependent characteristics of poly(3 hexylthiophene)-fullerene based heterojunction organic solar cells

Chirvase, D; Chiguvare, Z; Knipper, M; Parisi, J; Dyakonov, [No Value]; Hummelen, Jan

Published in:
Journal of Applied Physics

DOI:
10.1063/1.1545162

Temperature dependent characteristics of poly(3 hexylthiophene)-fullerene based heterojunction organic solar cells

D. Chirvase, Z. Chiguvare,[a] M. Knipper, J. Parisi, V. Dyakonov,[b] and J. C. Hummelen[c]
Energy and Semiconductor Research, University of Oldenburg, D-26111 Oldenburg, Germany

(Received 13 September 2002; accepted 17 December 2002)

Electrical and optical properties of poly(3-hexylthiophene-2.5diyl) (P3HT) used as the main component in a polymer/fullerene solar cell were studied. From the study of space-charge limited current behavior of indium-tin-oxide (ITO)/P3HT/Au hole-only devices, the hole mobility and density were estimated to range from 1.4×10^{-6} $cm^2/V\,s$ and 5.3×10^{14} cm^{-3} at 150 K to 8.5×10^{-5} $cm^2/V\,s$ and 1.1×10^{15} cm^{-3} at 250 K, respectively. The highest occupied to lowest occupied molecular orbital energetic difference was estimated from absorption spectrometry to be about 2.14 eV. Strong quenching of photoluminescence when the polymer was mixed with [6,6]-phenyl-C_{61} butyric acid methyl ester (PCBM), provided evidence of photoinduced charge transfer from P3HT to PCBM. Characterization of ITO/PEDOT:PSS/P3HT:PCBM/Al solar cells was done by analyzing the dependence of current density–voltage characteristics on temperature and illumination intensity. The main solar cell characteristics recorded at 300 K under 100 mW/cm^2 white-light intensity were: Open-circuit voltage 0.48 V, current density 1.28 mA/cm^2, with an efficiency of 0.2%, and fill factor of 30.6%. Open-circuit voltage decreased almost linearly with increasing temperature, while short circuit current density increased with temperature, saturating at around 320 K, and decreased thereafter. Power conversion efficiency and fill factor were maximum around 3 mW/cm^2 due to the poor bulk transport properties of the active layer. © *2003 American Institute of Physics.* [DOI: 10.1063/1.1545162]

I. INTRODUCTION

In the context of technological applications, among many conjugated polymers, poly(3-alkylthiophenes) have been found to be a special class of polymers with good solubility, processability, and environmental stability. Generally, this class of materials exhibits an optical band gap in the range of 1.7–2.1 eV.[1] Poly(para phenylene vinylene) (PPV), presently, the most intensively investigated candidate has a maximum of absorption at a wavelength spectrally mismatched to the sun's wavelength of maximum spectral irradiance, however, conversion efficiencies of between 1% and 2.5% for PPV based laboratory polymer/fullerene bulk heterojunction organic solar cells under standard test conditions (illumination intensity—1000 W/m^2 at normal incidence, AM 1.5 spectrum, and cell temperature 25 °C) have been reported.[2–4] An external quantum efficiency of only 10^{-4} has been reported for polythiophene based cells.[5]

In this article, we report the development of a bulk heterojunction polymer/fullerene solar cell based on regioregular poly (3, hexylthiophene-2,5diyl) (hereinafter referred to as P3HT), as an electron donor, and a soluble fullerene derivative [6,6]-phenyl-C_{61} butyric acid methyl ester (PCBM), as an electron acceptor.

Space-charge limited current (SCLC) measurements have been performed in order to determine the choice of electrodes and the bulk transport properties of the polymer. Optical properties of the polymer, like photoinduced absorption and photoluminescence were studied experimentally to establish the possibility of making a functional solar cell using this polymer. Electrical properties of the developed polymer/fullerene heterojunction solar cell have been investigated by recording the variation of current density–voltage ($J-V$) characteristics of the solar cell with light intensity and temperature.

The efficiency of solar cells depends on their capability for the absorption of photons, charge carrier generation, separation, and transport to the electrodes. Interpenetrating conjugated polymer-fullerene (donor-acceptor) networks, also referred to as bulk heterojunctions, are a very promising approach for the improvement of efficiency of polymer solar cells. Photovoltaic devices based on these interpenetrating networks provide increased charge carrier-generating interfaces, as compared to bilayer photovoltaic devices.

The general scheme of the charge carrier generation processes in nondegenerate conjugated polymers (without acceptor) can been described as follows: The mobile charge carriers responsible for the photocurrent are produced as a result of the dissociation of primarily generated singlet excitons due to interchain interaction, presence of oxygen,[6–8] or impurities.

Nevertheless, the charge carrier generation yield remains low, since other competitive processes, for example, photoluminescence and nonradiative recombination also occur. The carrier generation yield can be enhanced by the presence

[a]On leave from the Faculty of Engineering, University of Zimbabwe, P.O. Box MP167, Mount Pleasant, Harare, Zimbabwe.
[b]Author to whom correspondence should be addressed; electronic mail: dyakonov@uni-oldenburg.de
[c]Stratingh Institute and MSC, University of Groningen, Nijenborgh 4, 9747 AG Groningen, The Netherlands.

of a strong acceptor species, such as e.g., C_{60} molecule.[9] The process of charge separation in polymer/fullerene composites is ultrafast, and can occur within 40 fs in PPV/PCBM composites,[10] whereas the electron back transfer is much slower.[9] This results in effective formation of a metastable charge-separated state. The photoinduced charge transfer is dependent upon the electronic overlap of the donor (D)–acceptor (A) pair of molecules. A simple scheme for the charge electron transfer mechanism is as follows: First, the donor is excited, the excitation is delocalized on the D–A complex before charge transfer is initiated, leading to an ion radical pair and finally charge separation can be stabilized possibly by carrier delocalization on the D^+ (or A^-) species by structural relaxation[9]

$$D^* + A \rightarrow (D-A)^* \rightarrow (D^{+\cdot} - A^{-\cdot}) \rightarrow D^{+\cdot} - A^{-\cdot}. \qquad (1)$$

Electron transfer will only take place if the condition: $I_D^* - A_A - U_c < 0$ is satisfied locally, where I_D^* is the ionization potential of the excited state of the donor, A_A is the electron affinity of the acceptor, and U_c is the Coulomb energy of the separated radicals (including polarization effects). Stabilization of the charge separation can be enabled by carrier delocalization on the donor or acceptor species and by structural relaxation.

We add that the presence of a highly polar environment due to an electric field might assist this delocalization and facilitate general drift according to a Coulombic-type interaction. Such a ''field'' may result from the use of carefully selected electrode materials of different work functions. This selection is a very important step in the design of polymer–fullerene solar cells and will be described shortly. The properly chosen electrodes will selectively extract one type of charge carrier and block the other. Further, the accumulation of charges near the electrodes provides the voltage of the solar cell, while current will depend principally on the mobility of holes within the polymer and electrons within percolated fullerene networks.

The mechanism of charge transport has been proposed as follows: A polaronic-type radical cation is created due to the positive charge in the organic molecular material, and variable range hopping of this charge between adjacent polymer chains, or conjugated segments, generates the overall charge transport.[11–13] Many results such as those on the structure dependent conductivity and on field-effect transport between metal islands strongly support the model of hopping transport. In a similar way, it is assumed that the electrons are transported through the fullerene to the electrodes via a hopping mechanism.

The energetic picture of an ideal polymer/fullerene heterojunction solar cell, with the necessary electronic overlap, where there are no barriers at the electrode interfaces is proposed in Fig. 1. For the estimation of the limiting values of power conversion efficiency, η, open-circuit voltage, V_{oc}, short-circuit current, I_{sc}, and fill factor, FF, we propose the consideration of such a model. If that is the case, then highest-purity grade of materials should be assumed.

We note that in practice, even if all work functions (Fermi levels) were matched exactly to the highest occupied molecular orbital (HOMO) or lowest unoccupied molecular orbital (LUMO) levels, there exists a finite probability of having potential barriers at all the junctions possibly due to surface states, impurities adsorbed during junction formation, and possible chemical reactions between the materials contacted. In principle, these junctions operate like diodes. Further, it is very difficult to find compatible materials with any exact match of the necessary energy levels.

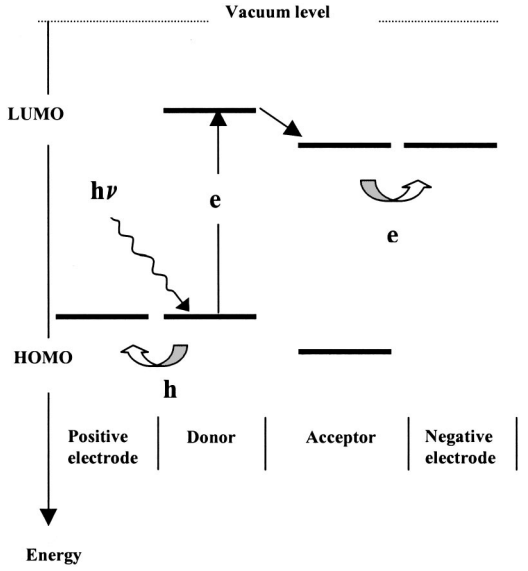

FIG. 1. Operation principle of an ideal polymer/fullerene heterojunction organic solar cell: Photons with energy $h\nu \geq E_{LUMO(D)} - E_{HOMO(D)}$ excite electrons into LUMO(D) which are then transferred to LUMO(A) from which they can be collected by negative electrode with work function equal to LUMO(A). Holes are collected by positive electrode with work function equal to HOMO(D).

For efficient charge collection from the absorber layer to an external circuit, both the positive and negative electrodes must form ohmic contacts with the donor and acceptor networks, respectively. If this is not the case, charge collection would be limited depending on the nature of potential barriers built up at the contacts. Analysis of the charge injection capability of an electrode into a polymer can yield conclusive results of whether a contact is ohmic or not.

We report the observation of SCLC behavior of hole-only Au/P3HT/indium tin oxide (ITO) devices and confirm the ohmic nature of the contacts between the ITO, Au, and the polymer. Further, we were able to determine the charge carrier density and the hole mobility in the polymer.

II. MATERIALS AND METHODS

Thin films of about 150 nm thickness were prepared by spin coating a chloroform-based solution of P3HT, on clean microscope slide glass substrates, in a nitrogen atmosphere of a glove box. Laser light of 457 nm of argon ion laser was used to excite the polymer and the photoluminescent spectrum was recorded by using a photodiode array detector. A solution of P3HT and PCBM was then prepared in the ratio 1:4 and the photoluminescent spectrum was recorded for films prepared in the same way as for pure P3HT samples. The absorption spectrum of a spin cast thin film was obtained by measuring the transmittance and reflectance of the

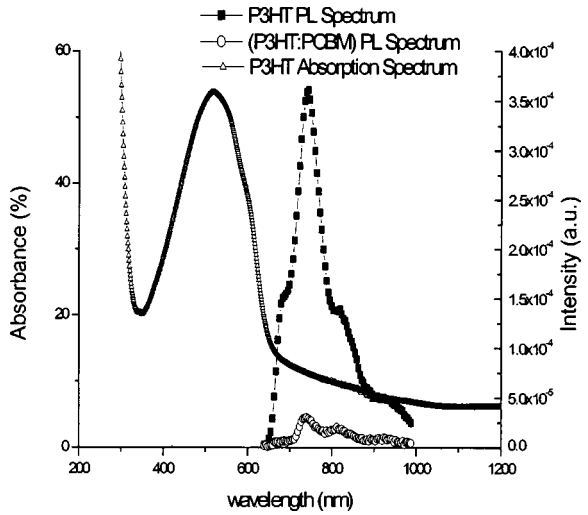

FIG. 2. Photoluminescence quenching is evidence of photoinduced charge transfer from P3HT to PCBM. The absorption spectrum of P3HT indicates an absorption edge at about 580 nm corresponding to a HOMO–LUMO energetic difference of 2.14 eV.

film using a Varian Carry 5E ultraviolet–visible-near-infrared spectrometer, and then subtracting their sum from 100%. The photoluminescent and absorption spectra are shown in Fig. 2.

ITO/P3HT/Au hole-only devices were prepared by spin coating P3HT from a chloroform solution, on clean ITO coated glass substrates in a nitrogen atmosphere of a glove box, and depositing Au contacts by thermal evaporation at low rate in a high vacuum (better than 10^{-6} mbar) in all cases. Preparation of devices of different thickness was realized by varying the speed of rotation of the spin coater. Temperature dependent, dark current–voltage measurements were performed in a vacuum of about 5×10^{-5} mbar in a liquid-nitrogen-cooled cryostat, using a source/measure unit (Advantest TR 6143). This step was necessary because the information concerning the HOMO–LUMO values of P3HT was not available to our knowledge, even from Sigma-Aldrich Chemie GmbH (Germany) from where the polymer was commercially available on a large scale. The large-scale availability of suitable materials is a prerequisite for the potential application of polymer solar cells; therefore, it is important to develop and test solar cells based on them. $J-V$ characteristics of the hole-only devices are shown in double logarithmic scale in Fig. 3.

ITO/PEDOT:PSS/P3HT:PCBM/Al heterojunction solar cells were prepared in a nitrogen atmosphere of a glove box and characterized. First, a thin layer of polyethylene-dioxythiophene doped with polystyrene-sulfonic acid (PEDOT:PSS) (Baytron P, Bayer AG, Germany) was spin coated (1500 rpm) on patterned clean ITO coated glass substrates in order to smoothen the surface of ITO and, hence, avoid possible short circuits due to the spiky roughness of the surface. PEDOT:PSS is known as a *p*-type semiconductor, a good hole transport material, and assures a better hole collection from the active layer onto the ITO electrode.

An active layer consisting of a mixture of P3HT/PCBM at a 1:4 mass ratio dissolved in a chloroform–toluene solvent

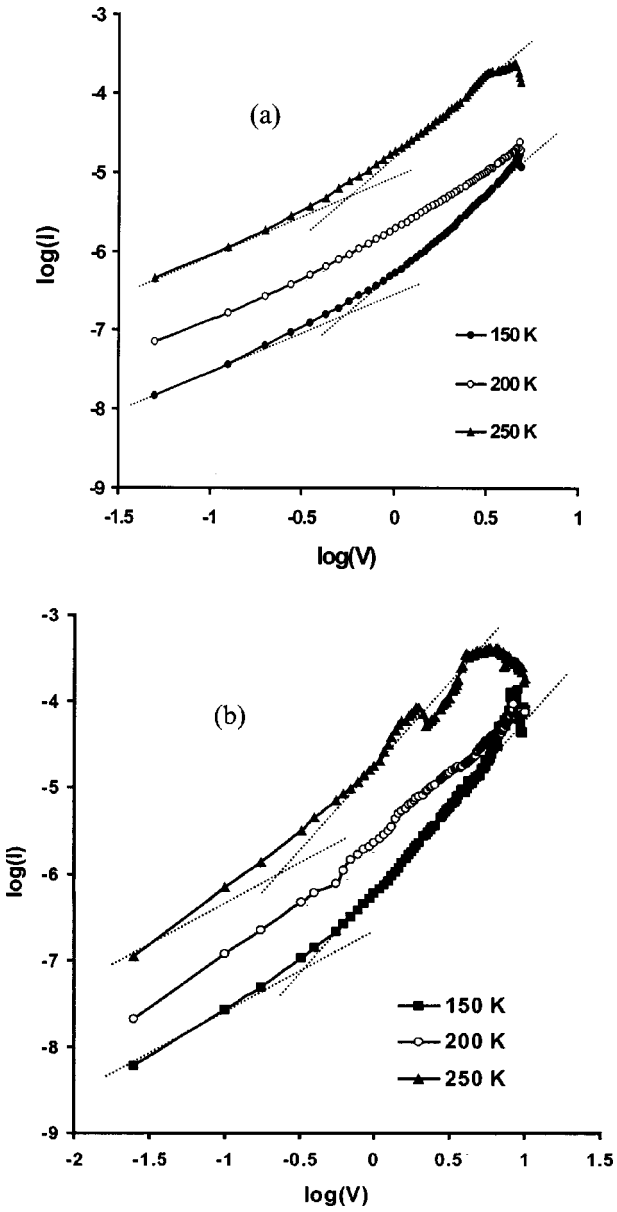

FIG. 3. Current–voltage curves for hole injection into P3HT through (a) Au and (b) ITO. Dotted lines show slope 1 and slope 2.

mixture at 0.25 wt % was then spin coated (speed 4000 rpm) on top of the dry PEDOT:PSS film to give a thin film of about 100 nm. Finally, 100 nm Al contacts were deposited on the active layer by thermal evaporation at low rate in a high vacuum of better than 1×10^{-6} mbar in all cases. The formulas of the materials forming the donor–acceptor heterojunction and the process of photoinduced electron transfer are shown in Fig. 4(a). The schematic of the designed solar cell is shown in Fig. 4(b).

Temperature and illumination dependent current–voltage characteristics were obtained by utilizing an Advantest TR 6143 source/measure unit, with the solar cell placed in a liquid-nitrogen-cooled cryostat at better than 10^{-5} mbar vacuum. A 150 W xenon lamp (Osram XB0 150W/XBR) was used as the illumination source with a water filter placed in the light path in order to approximate the AM1.5 solar spectrum. The light intensity reaching the device inside the

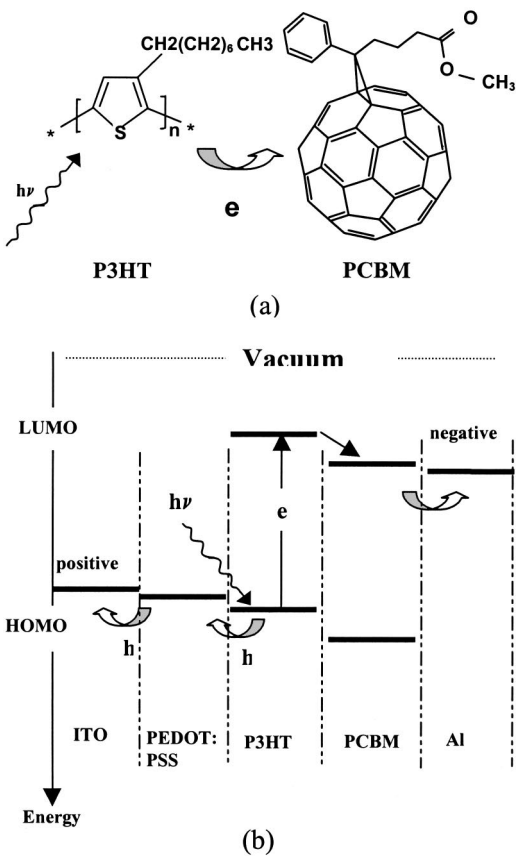

FIG. 4. (a) Formulas of the materials forming the donor acceptor heterojunction, (b) Operation principle: Photons with energy $h\nu \geqslant 2.14$ eV excite electrons from HOMO (P3HT) into LUMO (P3HT), which are then transferred to LUMO (PCBM), from which they can be collected by a Al electrode with work function $\phi \approx 4.2$ eV. Holes are collected, via PEDOT:PSS work function ≈ 5.0 eV, by +ve ITO electrode with work function ≈ 4.8 eV. (Possible recombination paths are not indicated in the diagram).

cryostat was calibrated to 100 mW/cm^2 and neutral density filters were used to vary the intensity by three orders of magnitude, i.e., from 0.1 to 100 mW/cm^2.

III. RESULTS AND DISCUSSION

A. Photoluminescence quenching in P3HT:PCBM composite

We have observed that P3HT exhibits photoluminescence, which is strongly (almost completely) quenched when the polymer is mixed with PCBM. Figure 2 shows the photoluminescence spectra of P3HT alone and also when mixed with PCBM. This photoluminescence quenching together with measurements of light-induced electron spin resonance and photoinduced absorption (not shown) provide evidence of photoinduced electron transfer in the P3HT/PCBM blend.

We have estimated the HOMO–LUMO energetic difference to be about 2.14 eV from an absorption spectrum of a spin cast thin film (Fig. 2), which corresponds to the midpoint of the absorption edge, at a wavelength of about 580 nm.

B. Current–voltage studies of ITO/P3HT/Au devices

The choice of electrodes was done after the analysis of current injection into hole-only ITO/P3HT/Au devices. Figure 3(a) shows typical curves of log(J) against log(V) plots obtained when injecting holes through the gold contact (higher potential on Au) and Fig. 3(b) shows the same but for injection through the ITO contact (higher potential on ITO). We note that the current at 150 K is lower than at 250 K.

The $J-V$ characteristics are nearly linear at low voltages and become superlinear at high voltages. In Fig. 3(a), the slope of the curve at low voltages is exactly one and at higher voltages it is exactly 2. The dotted lines have slopes 1 and 2, respectively. Superlinear $J-V$ behavior indicates the so-called SCLC where the electrode injects more holes than what the material can transport. The space-charge limited dark conduction (charge generation is not through light absorption or heat agitation) occurs when the contacting electrodes are capable of injecting either electrons into the conduction band or holes into the valence band of a semiconductor or an insulator, and when the initial rate of such carrier injection is higher than the rate of recombination, so that the injected carriers will form a space charge to limit the current flow.

SCLC's in a device can occur if at least one contact[13] is able to inject locally higher carrier densities than the material has in thermal equilibrium without carrier injection. Such a contact is referred to as ohmic. With ohmic contacts, the current voltage relation is often ohmic at low bias up to a certain value since the field due to the injected carriers is negligible compared to that due to the applied bias. This can be seen by a linear relation (slope 1 in log–log plot) between current I (or current density J), and voltage V at low voltages described by Eq. (2):[14]

$$J_{\text{ohm}} = q n_P \mu \frac{V}{d}, \tag{2}$$

where q is the electronic charge, n_p is the charge carrier density, μ is the carrier mobility, V is applied voltage, and d is thickness of sample. This condition breaks down at the space charge limit when the injected carrier density becomes so great that the field due to the carriers themselves dominates over that of the applied bias and then becomes space-charge limited. At this point, the $J-V$ characteristics should switch to pure SCLC flow for higher voltages. In the absence of traps, the trap free SCLC's situation can be observed, and the $J-V$ follows Child's law [see Eq. (3)]. This behavior is characterized by a strict quadratic dependence of current on voltage (slope 2) (Note that this does not necessarily imply the absence of traps in the material, but rather that they are all filled.)

$$J_{\text{SCL}} = \frac{9}{8} \varepsilon_o \varepsilon_r \mu \frac{V^2}{d^3}. \tag{3}$$

Here, ε_r and ε_0 are relative permittivity and permittivity of free space, respectively. If at higher applied bias the quasi-Fermi level intersects a trap distribution, e.g., exponential, then the characteristics will begin to follow Eq. (4):

$$J_{\mathrm{SCL}}=\frac{9}{8}\varepsilon_r\varepsilon_o\theta\mu\frac{V^2}{d^3}, \tag{4}$$

where θ is the fraction of the total charges free to move, which depend on the trap density and the activation energy to thermally excite a charge from the trap to the conduction band. Alternatively, if the trap distribution is energetically deep enough, the quasi-Fermi level may have already entered the trap distribution by the time the space-charge limit is reached. In that case, the characteristics will switch directly from ohmic to that of SCLC with an exponential distribution[15] or any other functional distribution as might adequately describe the traps.

It is also possible that the injected carrier density may be so great even at low applied bias that the ohmic regime is never observed. The initial $J-V$ characteristics then immediately follow pure SCLC flow. This appears to occur for ITO/dialcoxy PPV/Au positive carrier devices,[11,12] and as well for the ITO/P3HT junction of our device, where the slope equal to 1 is not observed, but starts as a slope between 1 and 2. Additionally, if there is charge carrier generation within the material, it manifests itself in the $J-V$ curves as a subohmic behavior, but the current is much higher in forward bias (or much lower in reverse bias) than could be possible with ohmic conduction.

Additionally the linear slope of the $J-V$ curve and, hence, the specific conductivity has to be independent of the film thickness. This is indicated by a thickness independent transition voltage from the linear to the quadratic dependence of the $J-V$ curve, which has been reported to be around 1 V for α-6Ts and even for compressed powders.[1,16] This requirement is satisfied in the case of our devices of different thickness, where the cross over voltage is about 1.0 V at 300 K.

We calculated hole mobilities and densities by equating Ohm's [Eq. (2)] and Child's [Eq. (3)] laws at cross over points indicated by the intersection of lines of slopes 1 and 2 in Fig. 3(a). The calculated hole mobility and density range from 1.4×10^{-6} cm^2/V s and 5.3×10^{14} cm^{-3} at 150 K to 8.5×10^{-5} cm^2/V s and 1.1×10^{15} cm^{-3} at 250 K, respectively, for a 465 nm film, where dielectric permittivity has been assumed to be 3. Additionally, the calculated hole mobility and density can be used for estimation of other electrical properties like the short-circuit current or open-circuit voltage, etc.

The $J-V$ behavior at voltages above 6 V could not be studied because above this voltage the device undergoes irreversible breakdown and its resistance increases by more than three orders of magnitude. It is worth mentioning that after this breakdown, which might be attributed to the burning out of shorts or local melting at the contact with the electrode, measurement shows similar shape of curves although with currents reduced by the same number of orders. For the same applied voltages, current increases with temperature indicating a negative temperature coefficient for the resistivity. The ITO contact does not show the slope$=1$ behavior at low voltages, indicating that the carrier density is very great even at low applied bias. Unfortunately, this behavior cannot be used to estimate this density, i.e., suffice it to say that Au is an ohmic contact and ITO provides an even better injection.

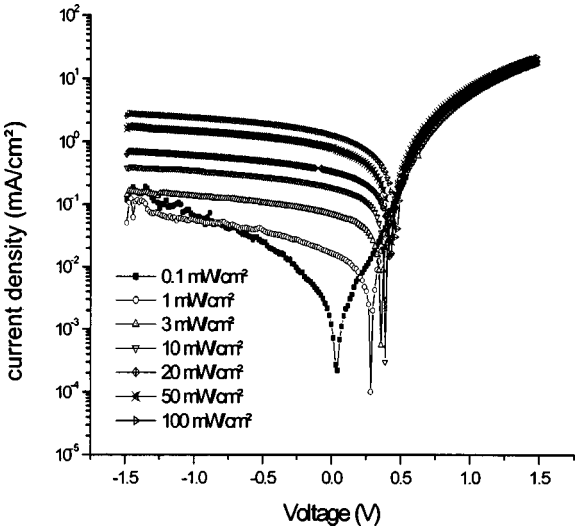

FIG. 5. $J-V$ characteristics of an ITO/PEDOT:PSS/P3HT:PCBM/Al solar cell at different illumination intensities 0.1–100 mW/cm^2 (white light). $T=300$ K.

C. Studies of ITO/PEDOT:PSS/P3HT:PCBM/Al solar cell

We turn now to solar cells. Typical $J-V$ characteristic curves of an ITO/PEDOT:PSS/P3HT:PCBM/Al solar cell have been plotted in a semilogarithmic representation in Fig. 5 at different light intensities from 0.1 to 100 mW/cm^2 at $T=300$ K. For this cell, values obtained for the main parameters such as power conversion efficiency, η, open-circuit voltage, V_{oc}, short-circuit current density, J_{sc}, and fill factor, FF, are shown in Table I. The dark $J-V$ characteristic curve (not shown) demonstrates typical diodelike behavior. The rectification is not due to the presence of a space-charge region as in a *p-n* junction (or alternatively, due to a Schottky contact), but possibly due to the work function difference of the two different electrode materials as well as the different mobility of electron and holes within the bicontinuous interpenetrating network of two components. Under illumination, the rectification ratio decreases from 200 at 0.1 to 10 at 100 mW/cm^2. This is a common feature of polymer solar cells, but the underlying reasons remain unclear.

TABLE I. Output characteristics of an ITO/PEDOT:PSS/P3HT:PCBM/Al solar cell.

P_{light} (mW/cm^2)	J_{sc} (mA/cm^2)	U_{oc} (V)	FF (%)	η (%)
100	1.280	0.480	30.6	0.188
50	0.807	0.450	33.9	0.246
20	0.335	0.420	37.0	0.260
10	0.189	0.405	38.0	0.291
3	0.070	0.360	39.7	0.332
1	0.016	0.300	33.7	0.166
0.1	0.012	0.045	20.0	0.108

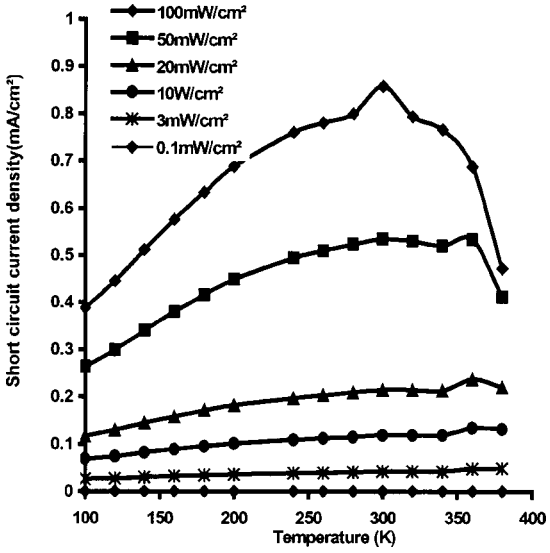

FIG. 6. Variation of the short-circuit current density with temperature.

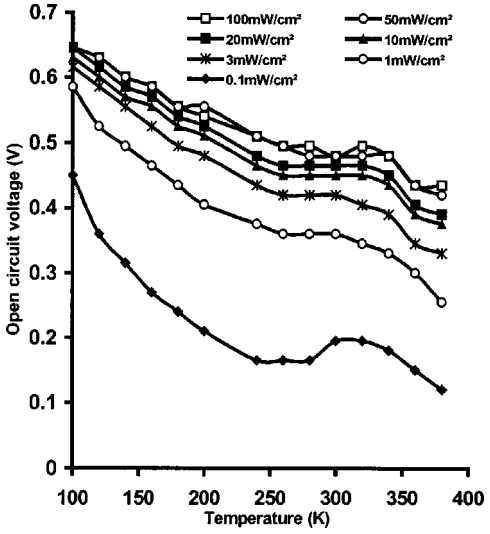

FIG. 7. Variation of open-circuit voltage with temperature.

We observed an increase of short-circuit current density with temperature, which tends to saturate to some maximum value around 300 K, followed by a decrease at higher temperature values as shown in Fig. 6. This can be understood by considering that the current output of a solar cell is proportional to the number of generated charge carriers and to their mobility. In most conventional inorganic semiconductors, mobility varies with temperature according to the following law:[1]

$$\mu \alpha T^{-n}, \tag{5}$$

where $n=3/2$ for impurity scattering and $n=-3/2$ for lattice scattering. In this case, the main mechanisms that influence electron and hole mobility are lattice scattering and impurity scattering. In lattice scattering, a carrier in a crystal is scattered by a vibration of the lattice dependent on the temperature. The frequency of such scattering events increases with the temperature since the thermal agitation of the lattice becomes greater. Therefore, we should expect the mobility to decrease as the sample is heated.

In organic semiconductors, there is another mechanism that determines the variation of the mobility of charge carriers. The charge transport occurs via localized states, where the tunneling of charges from one site to the next may be assisted by the phonons. The mobility is, therefore, thermally activated, i.e., it increases when the temperature increases. In this case, one should expect an increase of mobility with temperature according to the phonon activated hopping mechanism. This is justified by considering that for organic materials another law determines the conductivity:[17]

$$\sigma = \sigma_o \exp\left(-\frac{\Delta E}{2kT}\right), \tag{6}$$

and

$$\mu = \frac{\sigma}{zen}, \tag{7}$$

where σ is conductivity (Ω^{-1} cm^{-1}), ze is net charge of carriers, n is the concentration of charge carriers, and ΔE is the activation energy.

The activation energy has two contributions, the band gap values (energy necessary to excite electrons from HOMO to LUMO) and the energy to delocalize the charge carriers (energy necessary for an electron to escape from a trap). In organic materials, the delocalisation process can also be assisted by phonons. At low temperature, the probability to find a phonon of sufficient energy to facilitate a hop to the nearest site will be low. As the temperature increases, charge carrier mobility and, therefore, conductivity should also increase. As a general conclusion for organic materials, at low temperatures, few charge carriers are thermally generated and are not easily transported, therefore, the current without illumination is low.

The observed maximum of the short-circuit current at a temperature of about 300 K, can be explained by considering the geometrical structure of the conjugated polymer used. The polythiophene chain has a quasiplanar structure on a short-range and a helical conformation over a large number of repeat units corresponding to the minimum of intermolecular energy. The polymer film structure is built up by a packing of these helices. Conductivity is expected to be very sensitive to the chain conformation. At higher temperature, the quasiplanar structure of the polymer chain is changed by small twists of the monomer units, which leads to a decrease of the conductivity.[18] The aforementioned thermally activated hopping mechanism and the temperature dependent morphology alteration of the polymer are opposing processes which appear to give maximum of charge carrier mobility around room temperature.

The open-circuit voltage of a ITO/PEDOT:PSS/P3HT:PCBM/Al decreases almost linearly increasing the temperature from 80 to 300 K, as shown in Fig. 7. We make use of the model for conventional inorganic semiconductor solar cells to explain the obtained behavior of open-circuit voltage. For a *p-n* junction solar cell, the open-circuit voltage is given by

$$V_{oc}=\frac{kT}{e}\left(\ln\frac{I_{sc}}{I_0}+1\right)\approx\frac{kT}{e}\left(\ln\frac{I_{sc}}{I_0}\right), \tag{8}$$

where I_{sc} is short-circuit current, I_0 is reverse saturation current, k is Boltzmann's constant, T is absolute temperature, and e is the electronic charge.
Considering that

$$I_0=I_{0\,\max}\exp\left(-\frac{E_g}{kT}\right), \tag{9}$$

where E_g is the energy gap of the material, and substituting it in Eq. (8), we get

$$V_{oc}=\frac{E_g}{e}-\frac{kT}{e}\ln\frac{I_{0\,\max}}{I_{sc}}. \tag{10}$$

The variation of open-circuit voltage with temperature is shown in Fig. 7. The open-circuit voltage manifests an almost linear decrease with increase in temperature, consistent with inorganic solar cell theory. However, around 320 K, we observed a local maximum. The highest recorded open-circuit voltage value of 0.65 V was obtained at 100 K. Moreover, for all illumination intensities studied, the $V_{oc}(T)$ increases to a convergence point of 0.75 V that can be extrapolated for $T\rightarrow 0$ K. This voltage can be treated as an upper limit value for the device in question. The dependence can however not be completely linear, because the above aforementioned model even inorganic materials does not take into account the variation of the band gap with temperature,[19] which should follow Eq. (11)

$$E_g=E_{g,0}-\frac{aT^2}{b+T}, \tag{11}$$

where E_{g0} is the band gap at $T=0$ K, and a and b are constants. Katz *et al.*[2] have proposed a straight line equation to describe $V_{oc}(T)$ dependence, where they considered the energy gap to be independent of temperature. The matching of their proposed equation with experimental data suggests that the variation of the band gap with temperature might be negligible when compared to that of the second term on the right-hand side of Eq. (10).

As stated herein, we may conclude that the open-circuit voltage for our solar cells slightly exceeds the contact potential difference of respective electrodes (ITO/PEDOT:PSS and Al), which is 0.7 eV. Even higher deviations from that value are obtained for PPV:PCBM solar cells.[2] Therefore, we may conclude that the V_{oc} is determined by the energetic difference between the LUMO of the acceptor and the HOMO of the donor. This can be defined as a thermodynamic limit for the open-circuit voltage of donor–acceptor solar cell. This is a possible reason why the curves in Fig. 7 come closer to each other as the light intensity increases. This fact demonstrates saturation behavior and indicates that open-circuit voltage is an intrinsic property of the absorber material.

Curves that show the variation of the power conversion efficiency and fill factor with temperature and light intensity are shown in Figs. 8, 9, and 10, respectively. The efficiency η and fill factor FF have been calculated from the J–V curves according to

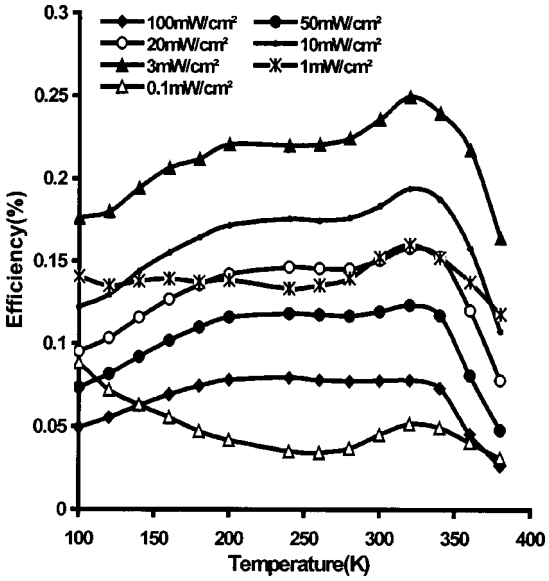

FIG. 8. Variation of efficiency with temperature.

$$\mathrm{FF}=\frac{V_{mpp}J_{mpp}}{V_{oc}J_{sc}}, \tag{12}$$

and

$$\eta=FF\,\frac{V_{oc}J_{sc}}{P_{light}}, \tag{13}$$

where V_{mpp}, J_{mpp} are voltage and current density at the maximum power point, respectively, and P_{light} is the illumination intensity in units of power/area.

From Figs. 8 and 9, we observe a maximum around 320 K temperature, resulting from the common adding effect of the open-circuit voltage and the short-circuit current. The fact that the maximum value of solar cell power conversion efficiency has been recorded at 3 mW/cm^2 (Fig. 10), may be attributed to the poor transport properties of the absorber, implying that although more charge carriers are photogener-

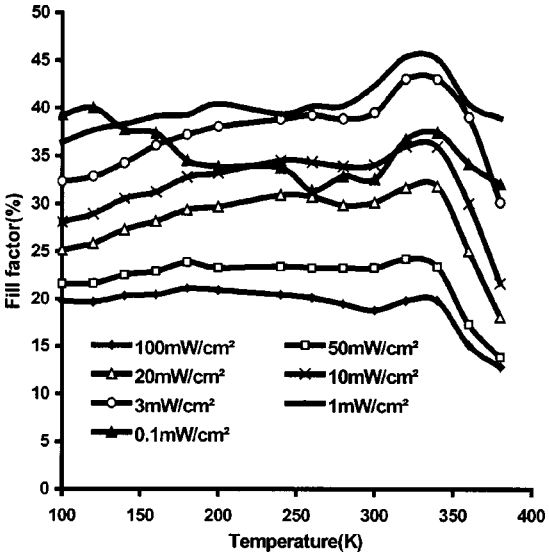

FIG. 9. Variation of fill factor with temperature.

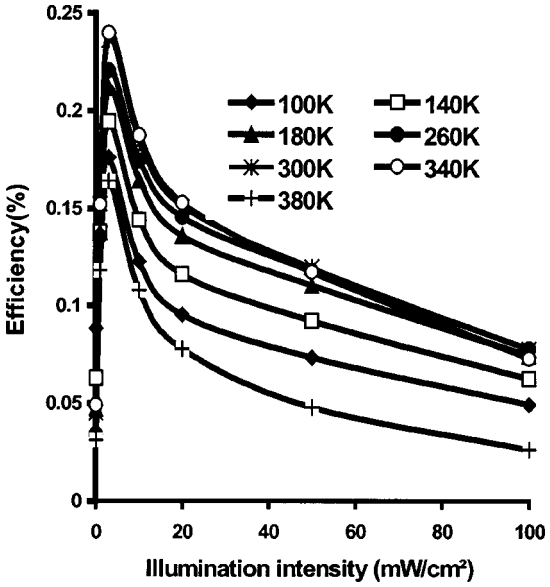

FIG. 10. Variation of efficiency with illumination intensity.

ated at higher light intensities, they cannot be easily transported to the electrodes. The same behavior has been reported in the literature for amorphous silicon solar cells. In the case of polythiophene, this effect might be a contribution of the highly disordered structure and possible phase separation between donor and acceptor, both resulting in low mobility of charge carriers. Apart from this, the purity of the polymer may strongly influence the output characteristics of the solar cells. Our P3HT showed strong electron spin resonance (dark) signals, clearly indicating presence of impurities. These may be results of residual catalysts used during the synthesis of the polymer.

IV. CONCLUSIONS

A configuration of an ideal donor/acceptor heterojunction solar cell that consists of an interpenetrating network of donor and acceptor as the absorber layer, sandwiched between a positive electrode with work function equal to the HOMO level of the donor, and a negative electrode with work function equal to the LUMO level of the acceptor, has been proposed. The SCLC studies of a hole-only device, showed that ohmic contacts can be obtained between ITO and P3HT. The energy gap of P3HT was estimated from absorption spectroscopy. A 0.2% efficient solar cell based on regioregular P3HT, as donor, and PCBM, as acceptor, has been fabricated and characterized by means of temperature and illumination dependent $J-V$ characteristics. We stress, however, the need of a homogeneous mixture of a donor and acceptor to ensure sufficient electronic overlap between molecules of the D–A blend, and propose an optimization of the mixture ratio and junction formation procedures that should eliminate any possibility of contact with oxygen or other contaminants, as possible ways of improving the efficiency of solar cells based on P3HT.

ACKNOWLEDGMENTS

Some of the authors (D.C., J.P., and V.D.) thank the EU-RTN Project EUROMAP run under HPRN-CT-00127. One author (Z.C.) thanks the GTZ and DAAD, for funding this research. They also thank I. Riedel, M. Pientka, D. Godovsky (all U of Oldenburg), and V. Zhokhavets (U of Ilmenau) for fruitful discussions and F. Voigt for assisting with absorption spectrometry. Acknowledgements also go to H. Holtorf, A. Geisler, and H. Koch (all U of Oldenburg) for technical support.

[1] D. Fichou, *Handbook of Oligo- and Polythiophene* (Wiley, New York, 1999).
[2] E. A. Katz, D. Faiman, S. M. Tuladhar, J. M. Kroon, M. M. Wienk, T. Fromherz, F. Padinger, C. J. Brabec, and N. S. Saricifci, J. Appl. Phys. **90**, 5343 (2001).
[3] S. E. Shaheen, C. J. Brabec, F. Padinger, T. Fromherz, J. C. Hummelen, and N. S. Sarifciftci, Appl. Phys. Lett. **78**, 841 (2001).
[4] M. Granström, K. Petritsch, A. C. Arias, A. Lux, M. R. Andersson, and R. H. Friend, Nature (London) **395**, 257 (1998).
[5] L. Sicot, C. Fiorini, A. Lorin, P. Raimund, C. Senterin, and J. M. Nunzi, Sol. Energy Mater. Sol. Cells **63**, 49 (2000).
[6] H. Antoniadis *et al.*, Phys. Rev. B **50**, 14911 (1994).
[7] S. Barth, H. Bässler, H. Rost, and H. H. Hörhold, Phys. Rev. B **56**, 3844 (1997).
[8] S. Barth and H. Bässler, Phys. Rev. Lett. **79**, 4445 (1997).
[9] N. S. Sariciftci, Prog. Quantum Electron. **19**, 131 (1995).
[10] C. J. Brabec, G. Zerza, N. S. Sariciftci, G. Cerullo, S. DeSilvesteri, S. Luzatti, and J. C. Hummelen, Chem. Phys. Lett. **340**, 232 (2001).
[11] P. W. M. Blom, M. J. M. de Jong, and J. J. M. Vleggaar, Appl. Phys. Lett. **68**, 3308 (1996).
[12] P. W. M. Blom, M. J. M. de Jong, and M. G. van Munster, Phys. Rev. B **55**, R656 (1997).
[13] W. Brütting, S. Berleb, and A. G. Mückl, Organ. Electron. **2**, 1 (2001).
[14] M. A. Lampert and P. Mark, *Current Injection into Solids* (Academic, New York, 1970).
[15] A. Campbell, D. D. Bradley, and D. G. Lidzey, J. Appl. Phys. **82**, 6326 (1997).
[16] S. Sen, P. Pal, S. Rossini, and T. N. Misra, J. Phys. Chem. Solids **55**, 17 (1994).
[17] J. Simon and J. J. Andre, *Molecular Semiconductors—Photoelectrical Properties and Solar Cells* (Springer, Berlin, 1985).
[18] A. Assadi, Appl. Phys. Lett. **53**, 195 (1988).
[19] S. M. Sze, *Semiconductor Devices* (Wiley, New York, 1985).